

## Article

# Innovative Investigation of Zinc Oxide Nanoparticles Used in Dentistry

Ajay Kumar Tiwari <sup>1</sup>, Saket Jha <sup>2</sup>, Abhimanyu Kumar Singh <sup>3,\*</sup>, Sheo Kumar Mishra <sup>4</sup>, Ashok Kumar Pathak <sup>5</sup>, Rudra Prakash Ojha <sup>6</sup>, Raghvendra Singh Yadav <sup>7</sup> and Anupam Dikshit <sup>2</sup>

<sup>1</sup> Department of Physics, Nehru Gram Bharati (Deemed to be University), Prayagraj 221505, India; ajayngbv@gmail.com

<sup>2</sup> Biological Product Laboratory, Department of Botany, University of Allahabad, Prayagraj 211002, India; jhasaket90@gmail.com (S.J.); anupambplau@gmail.com (A.D.)

<sup>3</sup> Department of Physics, Shyama Prasad Mukherjee Government Degree College, University of Allahabad, Prayagraj 211013, India

<sup>4</sup> Department of Physics, Indira Gandhi National Tribal University, Amarkantak 484886, India; sheokmishra@igntu.ac.in

<sup>5</sup> Department of Physics, Ewing Christian College, University of Allahabad, Prayagraj 211003, India; akpathak75@gmail.com

<sup>6</sup> Department of Zoology, Nehru Gram Bharati (Deemed to be University), Prayagraj 221505, India; drrudrapojha266@gmail.com

<sup>7</sup> Centre of Polymer Systems, Tomas Bata University in Zlin, Trida Tomase Bati 5678, 76001 Zlin, Czech Republic; yadav@utb.cz

\* Correspondence: abhimanyu.kr.singh@gmail.com



**Citation:** Tiwari, A.K.; Jha, S.; Singh, A.K.; Mishra, S.K.; Pathak, A.K.; Ojha, R.P.; Yadav, R.S.; Dikshit, A. Innovative Investigation of Zinc Oxide Nanoparticles Used in Dentistry. *Crystals* **2022**, *12*, 1063. <https://doi.org/10.3390/cryst12081063>

Academic Editor:  
Dinadayalane Tandabany

Received: 1 July 2022  
Accepted: 27 July 2022  
Published: 29 July 2022

**Publisher's Note:** MDPI stays neutral with regard to jurisdictional claims in published maps and institutional affiliations.



**Copyright:** © 2022 by the authors. Licensee MDPI, Basel, Switzerland. This article is an open access article distributed under the terms and conditions of the Creative Commons Attribution (CC BY) license (<https://creativecommons.org/licenses/by/4.0/>).

**Abstract:** Dental caries is a major lifestyle concern as dental components affect the face of an individual. The issue of tooth decay occurs in every age group throughout the globe. Researchers are probing incipient implements and techniques to develop filling agents for decayed teeth. Zinc oxide (ZnO) powder is utilized mostly as a filling agent. Nanotechnology enhanced the efficiency of compounds of metal oxides utilized for dental caries. The present study aims to investigate the properties of ZnO nanoparticles (NPs) synthesized chemically (using ZnCl<sub>2</sub> and NaOH) as well as biologically (using aqueous leaf extract of *Murraya paniculata*). The XRD patterns confirm that ZnO NPs have a hexagonal crystalline structure with particle sizes of 47 nm and 55 nm for chemically and biologically synthesized NPs, respectively. The FE-SEM data confirm the nanorod and spherical/cubical shape morphologies for the chemically and biologically synthesized ZnO NPs, respectively. FTIR data show the peaks between 4000 and 450 cm<sup>-1</sup> of the functional groups of -OH, C-O, -C-H-, and Zn-O bonds. The UV-Vis absorption study indicates a peak around 370 nm and a hump around 360 nm corresponding to the chemically and biologically synthesized ZnO NPs, respectively. An antibacterial bioassay was performed and compared with commercially available ZnO bulk powder against tooth decaying pathogens, viz., *Streptococcus mutans*, *Staphylococcus aureus*, *E. coli*, and *Lactobacillus fermentum*, and found that both ZnO NPs had results closer to those of the standard drug (rifampicin). Thus, the synthesized ZnO NPs may be utilized as nano-drugs for the application of tooth decaying filling agents. Even biologically synthesized ZnO NPs may be considered more environmentally friendly and less toxic to human health concerns.

**Keywords:** ZnO nanoparticles; dental caries; tooth decaying pathogens; antibacterial bioassay; broth microdilution; tooth filling agents

## 1. Introduction

Teeth play a generalized role in the individual personality. They not only help in verbalizing, but also affect one's countenance. Dental caries adversely affects an individual's personality and is a major concern in human welfare. Tooth decay is now becoming an incurable disease and is found to be a major concern for every age group. The people of

India and abroad are affected by this disease throughout their lifetime [1]. Researchers and medical practitioners are perpetually probing for novel concepts to deal with dental caries.

Cavities are created due to bacterial incursions as well as due to contingent causes, but there is always the pressure of having smooth and white teeth. Because of these exigencies, sundry tooth filling agents have been utilized as per their availability. These filling powders have always been regulated as they degrade and conventionally lack antibacterial properties. Several antibiotics have been used to cope with dental pathogens, but they have some limitations such as resistant microbes, antibiotic degradation, or loss of antimicrobial property [2]. The incorporation of nanotechnology resolves these issues and provides advanced implements and techniques for materials used as filling agents. Their nano-sized structure and sizably voluminous surface-to-volume ratio transmutes their properties compared with their bulk materials/compounds [3,4]. The bulk materials of calcium, silicon, gold, zinc, etc., have been widely utilized as filling agents and tooth implants.

Nanoparticles are considered to have more potential as they never lose their properties and are not degradable; however, they still need to be explored further due to health concerns [5–10]. Sundry applications have proved that these nanoparticles, associated with polymers [8] or having a surface coating [11,12], show maximum antimicrobial efficacy against tooth decaying pathogens [13–15]. Among several metal oxide nano-biomaterials, ZnO NPs have been found to be a good tooth filling agent; they are widely utilized because of their white color and because they show more antimicrobial properties [16–18]. These metal oxide nanoparticles protect from dental pathogens and never fade or become decolorized. Thus, a congruous implant with these nanoparticles provides a perpetual approach to tooth implantation and tooth fillings [19]. Their nano-sized structure provides the capability to enter inside the microbial cell membranes and facilely alter their metabolic pathways, leading to the death of or a decrease in microbial populations. The only difficulties with these nanoparticles are those regarding human health concerns. Many researchers believe that, due to their enhanced proprieties and nano-size, these nanoparticles may alter the biological metabolic pathways of human cells and lead to causing some cancers, rigorous diseases, or mutagenic irradiations [20].

Researchers are working on the establishment of nanoparticles with lesser toxicological activity against humans but that trigger more lethality towards pathogens. Many promising methodologies are being developed that still need to be further explored [21–30]. Simple methods were chemically synthesized with a hydrothermal decomposition reaction [31,32] and biologically with plant extracts, utilizing their secondary metabolites to minimize the size of the metal. These simple methods are convenient, environmentally friendly, and have a low cost [33,34].

In the present investigation, both biological and chemical synthesis techniques were performed to prepare ZnO NPs. Various characterization techniques, such as field emission scanning electron microscopy (FE-SEM), X-ray diffraction (XRD), Fourier transform infrared (FTIR) spectroscopy, and ultraviolet–visible (UV–Vis) spectroscopy, were used to evaluate their shape, particle size, bond stretching, and optical properties, respectively. Further, the synthesized ZnO NPs using a chemical method and a biological method were checked against major dental caries pathogens by utilizing the broth microdilution technique recommended by CLSI M7A8 [35]. Further, the antibacterial results of both the ZnO NPs were compared with the results of ZnO bulk powder.

## 2. Materials and Methods

### 2.1. Collection of ZnO Bulk Powder

The ZnO bulk powder (Dental products of India, Bombay Burmah Corporation Ltd., Mumbai, India) was collected from dentists of Sidhi Vinayak Dental Clinic at Naini, Prayagraj, India.

## 2.2. Chemical Synthesis of ZnO Nanoparticles

For the synthesis of ZnO NPs, an aqueous solution of 19.99 gm of sodium hydroxide (Merck, Mumbai, India) was integrated in the aqueous solution of 5.5 gm zinc chloride (Merck, Mumbai, India) with perpetual stirring (1200 rpm) at the temperature of 60 °C for 2 h. The white precipitate was filtered with Whatman filter paper no. 42, washed thrice with double distilled water, and left for 24 h in an oven at 200 °C [34,35]. Finally, the ZnO NPs were obtained in powder form.

## 2.3. Biological Synthesis of ZnO Nanoparticles

The preparation of ZnO NPs was performed as prescribed by Bela et al. [36] with some modifications. The 50 mL solution of zinc acetate (0.45 M) was integrated dropwise in the aqueous solution of 5 gm of leaves of *Murraya paniculata* with perpetual stirring (1200 rpm) at the temperature of 60 °C for 2 h. The precipitate was centrifuged at 6000 rpm for 15 min and washed thrice with ethanol and double distilled water. The brown color precipitate was kept for 24 h in a hot air oven at 100 °C. Finally, ZnO nanoparticles were obtained in powder form.

## 2.4. Inoculum Preparation

The tooth decaying pathogens were *Streptococcus mutans* (MTCC-497), *Staphylococcus aureus* (MTCC-3160), *Lactobacillus fermentum* (MTCC-1745), and *E. coli* (MTCC-723). The inocula were prepared from 24 h old cultures and the suspension was compared with 0.5 McFarland standard solution using a spectrophotometer at an optical density of 625 nm with a value of 0.08–0.13 as prescribed by CLSI guidelines [37]. The inoculants having a concentration of  $5 \times 10^5$  CFU/mL were utilized further for the broth microdilution technique for the drug susceptibility test.

## 2.5. Antibacterial Bioassay

The ZnO NPs synthesized by chemical as well as biological techniques and ZnO bulk powder were comparatively studied with their antibacterial property against tooth decaying pathogens, viz., *S. mutans*, *S. aureus*, *L. fermentum*, and *E. coli*. The broth microdilution method was performed to evaluate the antibacterial efficacy with standard protocol as prescribed by CLSI [35,37–42]. Rifampicin was taken as a standard drug and the assay was performed on 96-microtiter plates. The experimental plates were incubated at  $37 \pm 2$  °C in a BOD incubator for 24 h and data were calculated on a Spectramax Plus 384 molecular device.

## 3. Results and Discussion

The chemically and biologically synthesized ZnO NPs were characterized with X-ray diffractometer (Rikagu, Japan) for their crystalline sizes and structures, field emission scanning electron microscopy (FE-SEM) (Make: JEOL India Pvt. Ltd., Delhi, India) for their morphology, Fourier transform infrared (FTIR) spectrometer (Perkin Elmer, Buckinghamshire, UK) for their stability, and ultraviolet–visible (UV–Vis) spectrophotometer (Spectra Max, San Jose, CA, USA) for their optical properties; furthermore, the antibacterial property of ZnO NPs was assessed and compared with that of ZnO bulk powder (obtained from a dental clinic) against different bacterial strains.

### 3.1. X-ray Diffraction (XRD) Analysis of ZnO NPs

Figure 1a,b show the XRD patterns of ZnO NPs synthesized by chemical and biological methods, respectively. All peaks in Figure 1a,b matched with JCPDS Cat. No. 36-1451 and 79-0207 [43], confirming the formation of ZnO NPs. The XRD  $2\theta$  values were found for crystallography peaks at (100), (002), (101), (102), (110), (103), (200), (112), and (201) for the chemically as well as the biologically synthesized ZnO NPs. The grain sizes of XRD patterns were calculated from the Debye–Scherrer formula:

$$D = 0.9\lambda / \beta \cos\theta$$

where  $D$  is the grain size,  $\beta$  is the full width at half maximum (FWHM) in radians of the XRD pattern,  $\lambda$  is the X-ray wavelength, and  $\theta$  is the Bragg diffraction angle of the XRD peak. The particle sizes of the ZnO NPs synthesized by the chemical method (Figure 1a) and biological method (Figure 1b) were calculated from the above formula and found to be 47 nm and 55 nm, respectively, along with the high intensity orientation (002). Both NPs had hexagonal crystalline structures with space group P63mc (186). The appearance of some noise in the XRD pattern of the biologically synthesized NPs may be due to some impurities of other elements present in the leaves of *Murraya paniculata*.

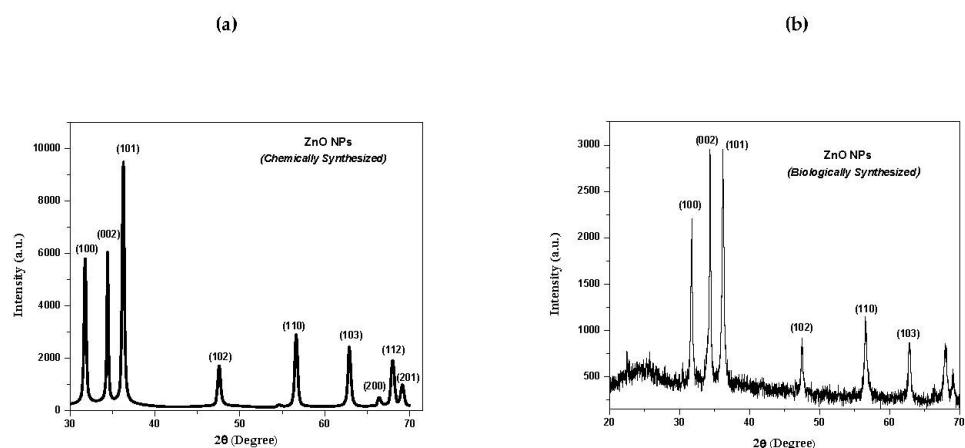


**Figure 1.** X-ray diffraction patterns of: (a) chemically synthesized ZnO NPs and (b) biologically synthesized ZnO NPs.

### 3.2. Field Emission Scanning Electron Microscopy (FE-SEM) Analysis of ZnO NPs

Figure 2a,b show FE-SEM images of ZnO NPs synthesized by chemical and biological methods, respectively. The FE-SEM images reveal the crystal shapes as being nanorods for the chemically synthesized ZnO NPs (Figure 2a) and spherical and cubical for the biologically synthesized ZnO NPs (Figure 2b). The thickness and length of the nanorods were calculated by the “image J” software as shown in the SEM image of Figure 2a. The thickness/diameter of the nanorods was 25–65 nm and the length of the nanorods was 250–600 nm. From the FE-SEM image of Figure 2a, it is clearly seen that the nanorods are uniformly distributed in the whole space. However, in the FE-SEM image of Figure 2b, it is clearly seen that the particle sizes vary from a very small size to a larger size and some particles are of spherical, cubical, and other shapes. There are clear differences in the morphology of the obtained nanoparticles by different synthesis methods. The formation of nanorods occurs by chemical reaction. In the case of biological synthesis, the processes of the formation of nanoparticles have a more complex mechanism than in the case of chemical synthesis.

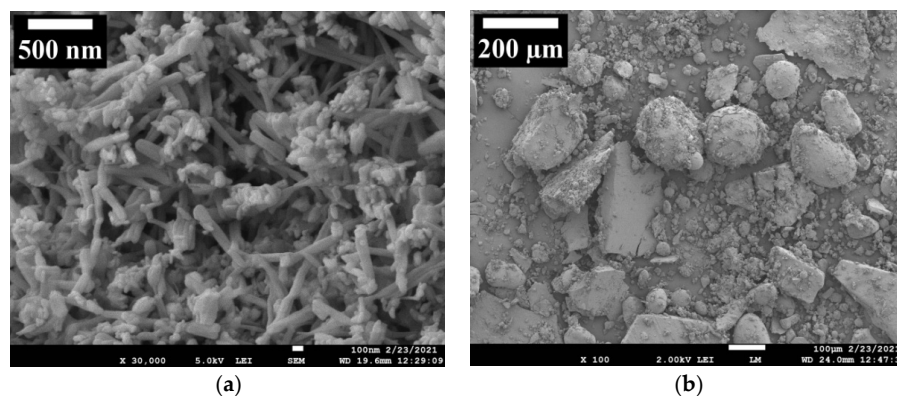


**Figure 2.** FE-SEM image of: (a) chemically synthesized ZnO NPs and (b) biologically synthesized ZnO NPs.

### 3.3. Fourier Transform Infrared (FTIR) Spectroscopy Analysis of ZnO NPs

Figure 3a,b show the FTIR spectra of ZnO NPs synthesized chemically and biologically, respectively. The FTIR spectra were recorded in the form of pellets utilizing spectroscopic grade KBr in the wave number range of 4000 to 450  $\text{cm}^{-1}$  in the diffuse reflectance mode. The spectrum of the chemically synthesized ZnO NPs (Figure 3a) showed bands of functional groups located at 3435, 2927, 2857, 1634, 1550, 1439, 1085, 1023, and 840  $\text{cm}^{-1}$ . The spectrum of the biologically synthesized ZnO NPs (Figure 3b) showed bands of functional groups located at 3427, 2934, 2854, 1568, 1420, 1340, 1022, 954, 694, 617, and 517  $\text{cm}^{-1}$ . The strong broad bands in the higher region at 3435 and 3427  $\text{cm}^{-1}$  are due to the stretching vibration of hydroxyl (OH) groups. The absorption bands at 2927, 2934, 2857, and 2854  $\text{cm}^{-1}$  are due to the stretching vibration of CH groups. The peaks around 1634, 1550, and 1568  $\text{cm}^{-1}$  correspond to the C=O amide group. The -C-H- bending vibration band arises at 1439, 1420, and 1340  $\text{cm}^{-1}$ . The C-O stretching vibration band arises at 1085, 1023, and 1022  $\text{cm}^{-1}$ . The peaks around 840, 954, and 694  $\text{cm}^{-1}$  are due to the bending vibration of =C-H groups. The peak around 617  $\text{cm}^{-1}$  is ascribed to the bending vibration of the O-H group. The absorption band at 517  $\text{cm}^{-1}$  is attributed to the stretching vibration of Zn-O bonds and confirms the formation of materials [44]. The peaks from 4000 to 450  $\text{cm}^{-1}$  observed in the spectra indicate the presence of -OH, C-O, and -C-H- residues, which may be due to the precursors used in the reaction.

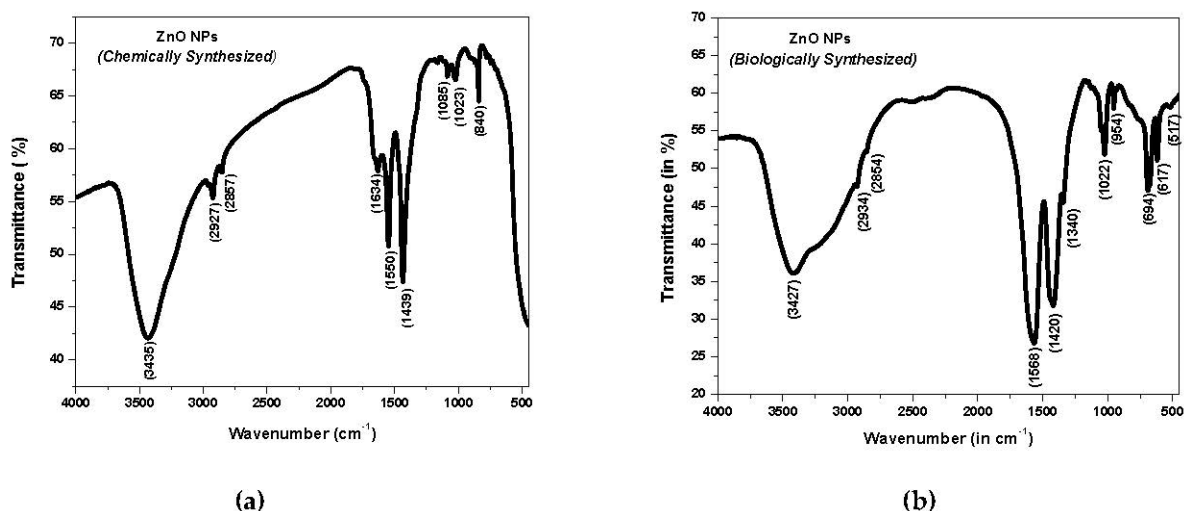


**Figure 3.** FTIR spectra of: (a) chemically synthesized ZnO NPs and (b) biologically synthesized ZnO NPs.

### 3.4. UV-Visible Spectroscopy Analysis of ZnO NPs

To explore the optical properties of the ZnO NPs, UV-visible spectroscopy is the best technique. The absorption spectrum of ZnO NPs is shown in Figure 4a,b. The high and stable peak found around 370 nm, corresponding to the chemically synthesized ZnO NPs (Figure 4a), confirms the formation of ZnO NPs. The hump around 360 nm, corresponding to the biologically synthesized ZnO NPs (Figure 4b), is evidence of the formation of ZnO NPs. The prepared ZnO nanoparticles exhibit an absorbance peak around 300 nm in Figure 1b, which corresponds to the formation of smaller-sized particles [45]. The smaller-sized particles are also seen in the SEM picture (Figure 2b), which also supports the above statement. It is also evidence that the paramount absorption of sharp ZnO NPs designates the mono-dispersed nature of the NPs distribution [43]. The average particle size of the ZnO NPs can be calculated from the UV-Vis absorption spectra using an effective mass model (Figure 3a,b) [46,47]. The band gap enlargement is expected for particle radii less than about 10 nm for biologically synthesized ZnO NPs and 20 nm for chemically synthesized ZnO NPs [48–50].

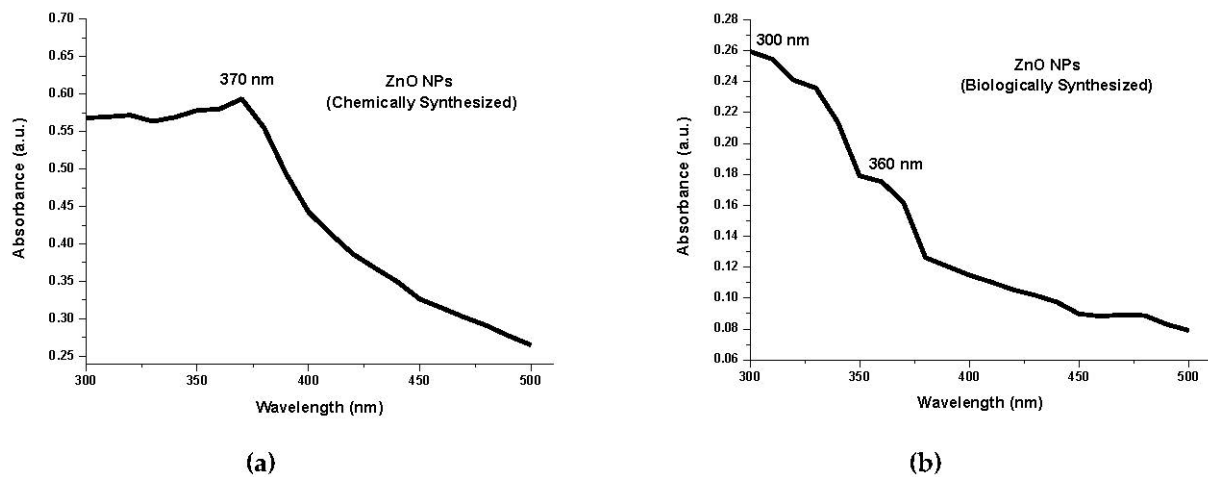


**Figure 4.** UV-Visible spectra of: (a) chemically synthesized ZnO NPs and (b) biologically synthesized ZnO NPs.

### 3.5. Antibacterial Bioassay of Synthesized ZnO NPs

The biologically synthesized ZnO NPs had minimum inhibitory concentration (MIC) values of 0.261  $\mu\text{g}/\text{mL}$  for *E. coli*, 0.293  $\mu\text{g}/\text{mL}$  for *S. mutans*, 0.134  $\mu\text{g}/\text{mL}$  for *S. aureus*, and 0.426  $\mu\text{g}/\text{mL}$  for *L. fermentum*. The chemically synthesized ZnO NPs were evaluated with MIC values of 0.193  $\mu\text{g}/\text{mL}$  for *E. coli*, 0.308  $\mu\text{g}/\text{mL}$  for *S. mutans*, 0.296  $\mu\text{g}/\text{mL}$  for *S. aureus*, and 0.407  $\mu\text{g}/\text{mL}$  for *L. fermentum*. Both the NPs were found to be more efficacious as compared to ZnO bulk powder. The biologically synthesized ZnO NPs were more efficacious against *S. mutans* and *S. aureus*, whereas the chemically synthesized ZnO NPs showed higher antibacterial efficacy against *E. coli* and *L. fermentum*. The MIC and half-maximal inhibitory concentration ( $\text{IC}_{50}$ ) values of both NPs were closer to the values of the standard drug rifampicin. Moreover, both NPs were found to be more effective compared to the ZnO bulk powder, leading to potency for the drug formulations against tested pathogens (Table 1, Figures 5 and 6a–d). Both nanomaterials were found to be much less effective against *S. mutans* and *L. fermentum* compared to the standard drug.

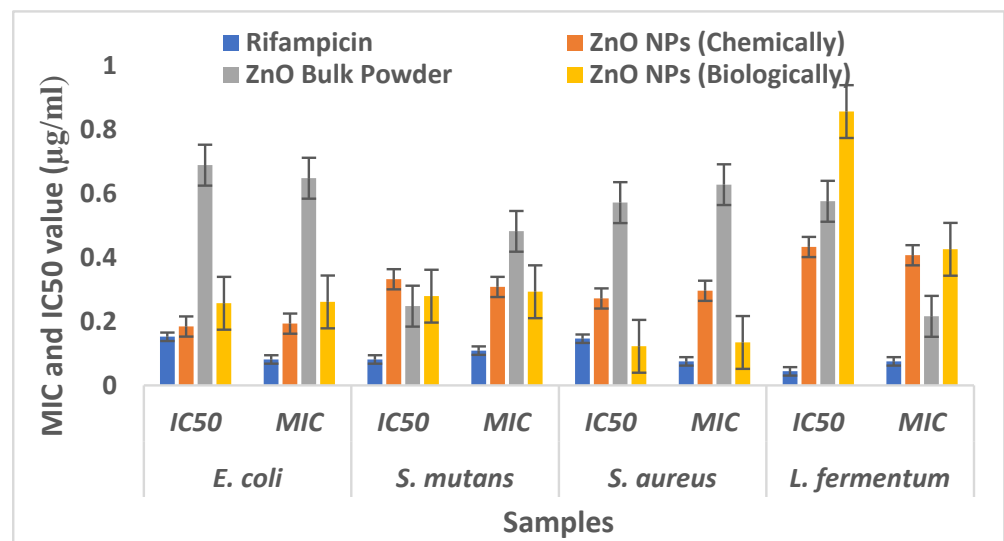


**Figure 5.** Comparative evaluation of antibacterial bioassay of synthesized ZnO NPs (chemically and biologically) with ZnO bulk powder against tooth decaying pathogens.

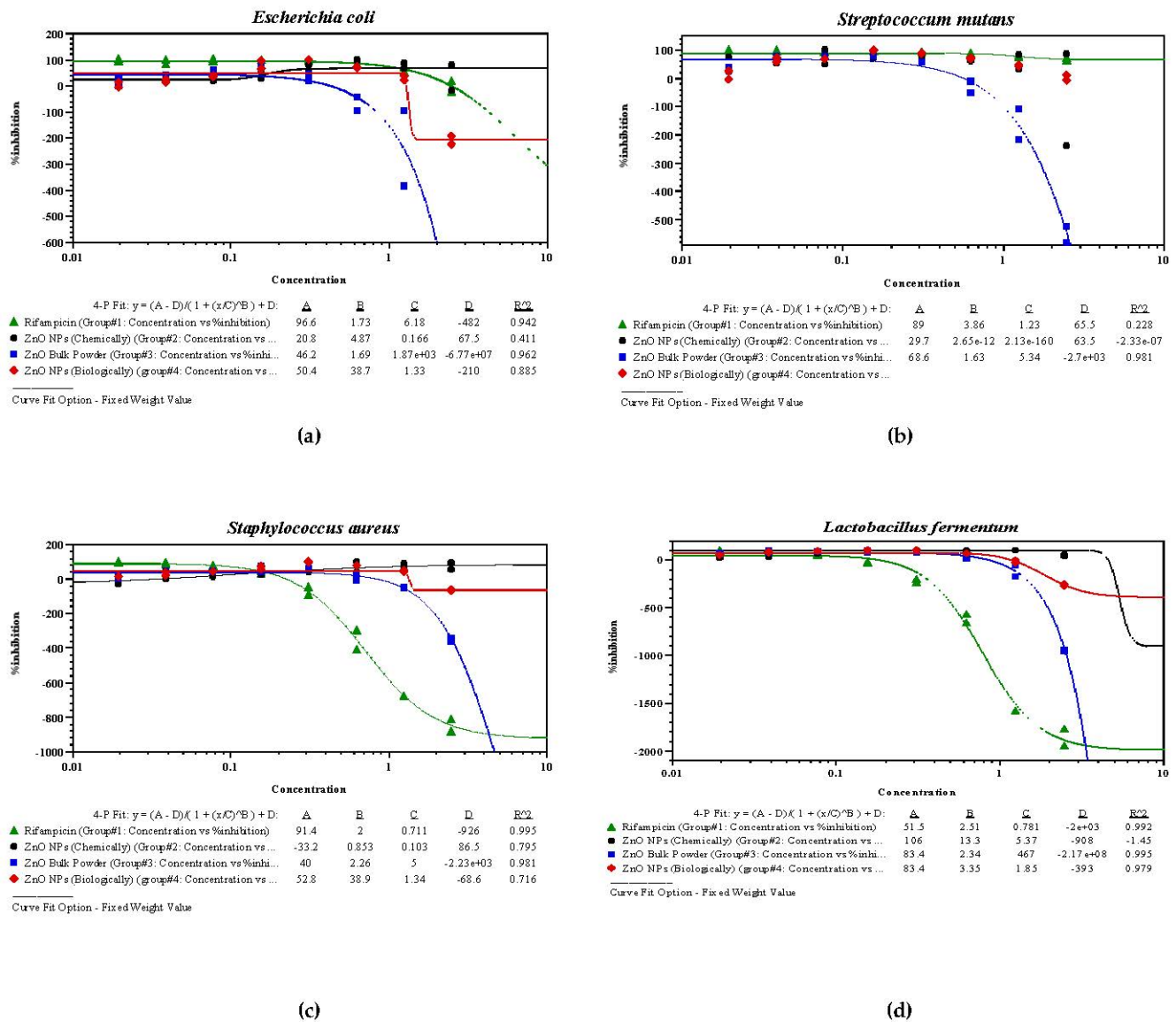


**Figure 6.** Antibacterial bioassay of synthesized ZnO NPs (chemically and biologically), ZnO bulk powder, and rifampicin against: (a) *E. coli*; (b) *S. mutans*; (c) *S. aureus*; and (d) *L. fermentum*.

**Table 1.** Antibacterial bioassay of synthesized ZnO NPs against tooth decaying pathogens.

S. No.	Drugs/ Samples	<i>E. coli</i>		<i>S. mutans</i>		<i>S. aureus</i>		<i>L. fermentum</i>	
		IC <sub>50</sub>	MIC	IC <sub>50</sub>	MIC	IC <sub>50</sub>	MIC	IC <sub>50</sub>	MIC
1	Rifampicin	0.152	0.081	0.081	0.108	0.146	0.075	0.044	0.075
2	ZnO NPs (chemically)	0.184	0.193	0.332	0.308	0.272	0.296	0.433	0.407
3	ZnO bulk powder	0.689	0.648	0.248	0.482	0.572	0.628	0.576	0.516
4	ZnO NPs (biologically)	0.257	0.261	0.279	0.293	0.122	0.134	0.457	0.426

Note: All the values are in MIC (in µg/mL) and IC<sub>50</sub> (in µg/mL).

Zinc has been widely used in human welfare since ancient times in the form of tooth powder and toothpaste [51,52]. Zinc has antibacterial properties and is a major constituent after calcium and magnesium in tooth formation. The present study was performed

with ZnO NPs and compared with commercially available ZnO bulk powder against tooth decaying pathogens utilizing the broth microdilution technique. The data were analyzed and found high antibacterial efficacy compared with the ZnO bulk powder [53,54]. The biologically synthesized ZnO NPs were found to have the highest antibacterial property against *S. aureus* and were less effective against *L. fermentum*. The chemically synthesized ZnO NPs were found to have more lethality against *E. coli* and were less toxic to *S. aureus*. Both nano-biomaterials were found to have a potential antibacterial property compared to the standard drug (rifampicin) and ZnO bulk powder. The antibacterial properties of ZnO NPs were also reported by other researchers [53–55]. The MIC values of the ZnO NPs synthesized chemically as well as biologically were found to be similar to those from other, earlier reports [56]. For the herbal (phyto)synthesis, more bioactive components were found and they showed less toxicity to human health [56,57]. Some researchers reported mechanisms wherein these nanoparticles trigger the release of free radicals which rupture the microbial cell membranes, causing their death [57,58]. Both synthesized ZnO NPs showed better proximity to the standard drug compared to ZnO powder against all four bacterial species. This may be due to the ZnO NPs having highly penetrable, large surface areas and stable properties compared to the ZnO bulk powder. The nano form of ZnO leads to alteration in cell membrane permeability, which is responsible for leakage of the components of the intracellular compartment [59,60].

#### 4. Conclusions

ZnO nanoparticles were successfully synthesized by chemical as well as biological methods. Biological synthesis of ZnO NPs using the aqueous leaf extract of *Murraya paniculata* as a reducing agent provides an environmentally friendly, simple, and efficient route for the synthesis of nanoparticles. The XRD patterns confirm that ZnO NPs have a hexagonal crystalline structure with space group P63mc (186). The particle sizes were found to be 47 nm and 55 nm for the chemically and biologically synthesized ZnO NPs, respectively, along with the high intensity orientation (002). FE-SEM data confirm the rod shape morphology with a thickness of ~25–65 nm and length of ~250–600 nm for the chemically synthesized ZnO NPs and spherical and cubical shapes for the biologically synthesized ZnO NPs. FTIR data show that the peaks between 4000 and 450  $\text{cm}^{-1}$  observed in the spectra indicate the presence of the functional groups –OH, C–O, and –C–H-. The absorption band at 517  $\text{cm}^{-1}$  is attributed to the stretching vibration of Zn–O bonds, which confirms the formation of materials for the biologically synthesized ZnO NPs. The UV–Vis absorption spectra of the ZnO NPs indicate that the high and stable peak was found around 370 nm, corresponding to the chemically synthesized ZnO NPs, which confirms the formation of ZnO NPs. The hump around 360 nm, corresponding to the biologically synthesized ZnO NPs, is evidence of the formation of ZnO NPs, and an absorbance peak around 300 nm corresponds to the formation of smaller-sized particles. Both ZnO NPs and ZnO bulk powder were comparatively studied with their antibacterial property with the broth microdilution method. The MIC and IC50 values of both the synthesized ZnO NPs showed better proximity to the values of the standard drug compared to those of the ZnO powder against tooth decaying pathogens, i.e., *S. mutans*, *S. aureus*, *L. fermentum*, and *E. coli*. This may be due to the ZnO NPs having a highly penetrable, large surface area and stable properties compared to the ZnO bulk powder. The present study has potentially shown the antibacterial efficacy of ZnO NPs against major tooth decaying pathogens, opening the door for biologically synthesized ones as an alternative that is more cost-effective and less toxic to human health. Finally, we conclude that the present study focused on the environmentally friendly and low-cost synthesized nanomaterials of other tooth filling elements, such as Ti, Ag, and Ca, which may be utilized as filling agents with high antibacterial efficacy. Moreover, the amalgamation of tooth filling nanomaterial powder can be further utilized in dentistry as well as other pharmacological applications. This study is helpful and useful to the scientific community for using ZnO NPs in dentistry, antimicrobial, and other pharmacological applications for commercial biomedical applications.

**Author Contributions:** Experimental design and data evaluated by A.K.T., S.K.M. and S.J.; discussion and data compiling by A.K.S., A.K.P., R.P.O., R.S.Y. and A.D. All authors have read and agreed to the published version of the manuscript.

**Funding:** This research received no external funding.

**Institutional Review Board Statement:** Not applicable.

**Informed Consent Statement:** Not applicable.

**Data Availability Statement:** Data will be made available upon request.

**Acknowledgments:** Authors are thankful to the director Subodh Kumar, Birbal Sahni Institute of Paleoscience, Lucknow, for SEM and valuable suggestions; R. R. Awasthi, Lucknow University for XRD; V. Bhadoria, Ewing Christian College, University of Allahabad for FTIR; the Head of the Department of Botany, University of Allahabad for providing the lab facility and UGC, New Delhi for financial Assistance to Anupam Dikshit as BSR Faculty.

**Conflicts of Interest:** The authors declare no conflict of interest.

## References

1. Selwitz, R.H.; Ismail, A.I.; Pitts, N.B. Dental caries. *Lancet* **2007**, *369*, 51–59. [[CrossRef](#)]
2. Aviv, M.; Berdicevsky, I.; Zilberman, M. Gentamicin-loaded bioresorbable films for prevention of bacterial infections associated with orthopedic implants. *J. Biomed. Mater. Res. A* **2007**, *83*, 10–19. [[CrossRef](#)] [[PubMed](#)]
3. Bonzonga, J.C.J.; Kopelevich, D.; Bitton, G. *Assessment of the Environmental Impacts of Nanotechnology on Organisms and Ecosystems*; Progress Report; United States Environmental Protection Agency: Washington, DC, USA, 2007.
4. Buzea, C.; Pacheco, I.I.; Robbie, K. Nanomaterials and nanoparticles: Sources and toxicity. *Biointerphases* **2007**, *2*, MR17–MR71. [[CrossRef](#)] [[PubMed](#)]
5. Cho, E.J.; Holback, H.; Liu, K.C.; Abouelmagd, S.A.; Park, J.; Yeo, Y. Nanoparticle characterization: State of the art, challenges, and emerging technologies. *Mol. Pharm.* **2013**, *10*, 2093–2110. [[CrossRef](#)]
6. Ramos, A.P.; Cruz, M.A.E.; Tovani, C.B.; Ciancaglini, P. Biomedical applications of nanotechnology. *Biophys. Rev.* **2017**, *9*, 79–89. [[CrossRef](#)]
7. Sirelkhatim, A.; Mahmud, S.; Seeni, A.; Kaus, N.H.M.; Ann, L.C.; Bakhori, S.K.M.; Hasan, H.; Mohamad, D. Review on zinc oxide nanoparticles: Antibacterial activity and toxicity mechanism. *Nano-Micro Lett.* **2015**, *7*, 219–242. [[CrossRef](#)]
8. Saafan, A.; Zaazou, M.H. Assessment of Photodynamic Therapy and Nanoparticles Effects on Caries Models. *Maced. J. Med. Sci.* **2018**, *6*, 1289–1295. [[CrossRef](#)]
9. Cao, W.; Zhang, Y. Development of a novel resin-based dental material with dual biocidal modes and sustained release of Ag<sup>+</sup> ions based on photo-curable core-shell AgBr/cationic polymer nanocomposites. *J. Mater. Sci. Mater. Med.* **2017**, *28*, 103. [[CrossRef](#)]
10. Magalhaes, A.P.; Moreira, F.C. Silver nanoparticles in resin luting cements: Antibacterial and Physiochemical properties. *J. Clin. Exp. Dent.* **2016**, *8*, 415–422. [[CrossRef](#)]
11. McNamara, K.; Tofail, S.A.M. Nanoparticles in biomedical applications. *Adv. Phys.* **2017**, *2*, 54–88. [[CrossRef](#)]
12. Madubuonu, N.; Aisida, S.O.; Ali, A.; Ahmad, I.; Zhao, T.K.; Botha, S.; Maaza, M.; Ezema, F.I. Biosynthesis of iron oxide nanoparticles via a composite of *Psidiumguavaja-Moringaoleifera* and their antibacterial and photocatalytic study. *J. Photochem. Photobiol. B Biol.* **2019**, *119*, 111601. [[CrossRef](#)]
13. Aisida, S.O.; Akpa, P.A.; Ahmad, I.; Zhao, T.-K.; Maaza, M.; Ezema, F.I. Bio-inspired encapsulation and functionalization of iron oxide nanoparticles for biomedical applications. *Eur. Polym. J.* **2020**, *122*, 109371. [[CrossRef](#)]
14. Cao, W.; Zhang, Y. Novel resin-based dental material with anti-biofilm activity and improved mechanical property by incorporating hydrophilic cationic copolymer functionalized nanodiamond. *J. Mater. Sci. Mater. Med.* **2018**, *29*, 162. [[CrossRef](#)]
15. Kasraei, S.; Sami, L. Antibacterial properties of composite resins incorporating silver and zinc oxide nanoparticles on *Streptococcus mutans* and *Lactobacillus*. *Restore. Dent. Endod.* **2014**, *39*, 109–114. [[CrossRef](#)]
16. Fernandes, G.L.; Delbem, A.C.B. Nanosynthesis of Silver-Calcium Glycerophosphate: Promising Association against Oral Pathogens. *Antibiotics* **2018**, *7*, 52. [[CrossRef](#)]
17. Fang, M.; Chen, J.H.; Xu, X.L.; Yang, P.H.; Hildebrand, H.F. Antibacterial activities of inorganic agents on six bacteria associated with oral infections by two susceptibility tests. *Int. J. Antimicrob. Agents* **2006**, *27*, 513–517. [[CrossRef](#)]
18. Burguera-Pascu, M.; Rodríguez-Archilla, A.; Baca, P. Substantivity of zinc salts used as rinsing solutions and their effect on the inhibition of *Streptococcus mutans*. *J. Trace Elem. Med. Biol.* **2007**, *21*, 92–101. [[CrossRef](#)]
19. Sevinc, B.A.; Hanley, L. Antibacterial activity of dental composites containing zinc oxide nanoparticles. *J. Biomed. Mater. Res.* **2011**, *94*, 22–31.
20. Jiang, J.; Pi, J.; Cai, J. The advancing of zinc oxide nanoparticles for biomedical applications. *Bioinorg. Chem. Appl.* **2018**, *2018*, 1062562. [[CrossRef](#)]
21. Tokumoto, M.S.; Pulcinelli, S.H.; Santilli, C.V.; Briois, V. Catalysis and temperature dependence on the formation of ZnO nanoparticles and of zinc acetate derivatives prepared by the sol-gel route. *J. Phys. Chem. B* **2003**, *107*, 568–574. [[CrossRef](#)]

22. Singhal, M.; Chhabra, V.; Kang, P.; Shah, D.O. Synthesis of ZnO nanoparticles for varistor application using Znsubstituted aerosol OT microemulsion. *Mater. Res. Bull.* **1997**, *32*, 239–247. [[CrossRef](#)]
23. Rataboul, F.; Nayral, C.; Casanove, M.J.; Maisonnat, A.; Chaudret, B. Synthesis and characterization of monodisperse zinc and zinc oxide nanoparticles from the organometallic precursor  $[Zn(C_6H_{11})_2]$ . *J. Organomet. Chem.* **2002**, *643*, 307–312. [[CrossRef](#)]
24. Okuyama, K.; Lenggoro, W.W. Preparation of nanoparticles via spray route. *Chem. Eng. Sci.* **2003**, *58*, 537–547. [[CrossRef](#)]
25. Moghaddam, A.B.; Nazari, T.; Badraghi, T.J.; Kazemzad, M. Synthesis of ZnO nanoparticles and electrodeposition of polypyrrole/ZnO nanocomposite film. *Int. J. Electrochem. Sci.* **2009**, *4*, 247–257.
26. Wei, Y.L.; Chang, P.C. Characteristics of nano zinc oxide synthesized under ultrasonic conditions. *J. Phys. Chem. Solids* **2008**, *69*, 688–692. [[CrossRef](#)]
27. Hu, X.L.; Zhu, Y.J.; Wang, S.W. Sono-chemical and microwave-assisted synthesis of linked single-crystalline ZnO rods. *Mater. Chem. Phys.* **2004**, *88*, 421–426. [[CrossRef](#)]
28. Wu, J.J.; Liu, S.C. Low-temperature growth of well-aligned ZnO nanorods by chemical vapor deposition. *Adv. Mater.* **2002**, *14*, 215–218. [[CrossRef](#)]
29. Zhai, H.J.; Wu, W.H.; Lu, F.; Wang, H.S.; Wang, C. Effects of ammonia and cetyl-trimethyl-ammonium bromide (CTAB) on morphologies of ZnO nano- and micro-materials under solvothermal process. *Mater. Chem. Phys.* **2008**, *112*, 1024–1028. [[CrossRef](#)]
30. Bitenc, M.; Marinsek, M.; Crnjak, O.Z. Preparation and characterization of zinc hydroxide carbonate and porous zinc oxide particles. *J. Eur. Ceram. Soc.* **2008**, *28*, 2915–2921. [[CrossRef](#)]
31. Ajmal, H.M.S.; Khan, F.; Nam, K.; Kim, H.Y.; Kim, S.D. Ultraviolet Photodetection Based on High-Performance Co-Plus-Ni Doped ZnO Nanorods Grown by Hydrothermal Method on Transparent Plastic Substrate. *Nanomaterials* **2020**, *10*, 1225. [[CrossRef](#)]
32. Ajmal, H.M.S.; Khan, F.; Huda, N.U.; Lee, S.; Nam, K.; Kim, H.Y.; Eom, T.-H.; Kim, S.D. High-Performance Flexible Ultraviolet Photodetectors with Ni/Cu-Codoped ZnO Nanorods Grown on PET Substrates. *Nanomaterials* **2019**, *9*, 1067. [[CrossRef](#)] [[PubMed](#)]
33. Westermarck, K.; Rensmo, H.; Siegbahn, H.; Keis, K.; Hagfeldt, A.; Ojamäe, L.; Persson, P. PES studies of Ru (dcbpyH<sub>2</sub>)<sub>2</sub> (NCS)<sub>2</sub> adsorption on nanostructured ZnO for solar cell applications. *J. Phys. Chem. B* **2002**, *106*, 10102–10107. [[CrossRef](#)]
34. Luna, I.Z.; Hilary, L.N.; Chowdhury, A.M.S.; Gafur, M.A.; Khan, N.; Khan, R.A. Preparation and Characterization of Copper Oxide Nanoparticles Synthesized via Chemical Precipitation Method. *Open Access Libr. J.* **2015**, *2*, 1409. [[CrossRef](#)]
35. Jha, S.; Singh, R.; Pandey, A.; Bhardwaj, M.; Tripathi, S.K.; Mishra, R.K.; Dikshit, A. Bacterial toxicological assay of calcium oxide nanoparticles against some plant growth-promoting rhizobacteria. *Int. J. Res. Appl. Sci. Eng. Technol.* **2018**, *6*, 460–466.
36. Bala, N.; Saha, S.; Chakraborty, M.; Maiti, M.; Das, S.; Basu, R.; Nandy, P. Green synthesis of zinc oxide nanoparticle using *Hibiscus subdariffa* leaf extract: Effect of temperature on synthesis, antibacterial activity, and antidiabetic activity. *RSC Adv.* **2015**, *5*, 4993–5003. [[CrossRef](#)]
37. Clinical and Laboratory Standards Institute (CLSI). *Methods for Dilution Antimicrobial Susceptibility Tests for Bacteria that Grow Aerobically Approved Standard*, 8th ed.; CLSI: Wayne, PA, USA, 2009.
38. Cos, P.; Vlietinck, A.J.; Berghe, D.V.; Maes, L. Anti-infective potential of natural products: How to develop a stronger in vitro “proof-of-concept”. *J. Ethnopharmacol.* **2006**, *106*, 290–302. [[CrossRef](#)]
39. Novy, P.; Kloucek, P.; Rondevaldova, J.; Havlik, J.; LenkaKourimska, L.; Kokoska, L. Thymoquinone vapor significantly affects the results of *Staphylococcus aureus* sensitivity tests using the standard broth microdilution method. *Fitoterapia* **2014**, *94*, 102–107. [[CrossRef](#)]
40. Singh, R.; Jha, S.; Pandey, A.; Dikshit, A.; Mishra, R.K. Comparison of Antibacterial Activities of essential oils of *Juniperus-communis*L., *Pinusroxburghii* Sarg. and *Taxodiumdistichum* L. against *Klebsiellapneumoniae*. *J. Emerg. Technol. Innov. Res.* **2018**, *5*, 661–669.
41. Tripathi, S.K.; Singh, R.; Jha, S.; Pandey, A.; Dikshit, A. Comparison of antibacterial activities leaf extracts of *Eclipta alba* against *Klebsiellapneumoniae*. *J. Emerg. Technol. Innov. Res.* **2018**, *5*, 349–352.
42. Khoshhesab, Z.M.; Sarfaraz, M.; Asadabad, M.A. Preparation of ZnO nanostructures by chemical precipitation method. *Synth. React. Inorg. Met. Nano-Metal Chem.* **2011**, *41*, 814–819. [[CrossRef](#)]
43. Talam, S.; Karumuri, S.R.; Gunnam, N. Synthesis, Characterization, and Spectroscopic Properties of ZnO Nanoparticles. *ISRN Nanotechnol.* **2012**, *2012*, 372505. [[CrossRef](#)]
44. Jayarambabu, N.; Kumari, S.; Rao, K.V.; Prabhu, Y.T. Germination and Growth Characteristics of Mungbean Seeds (*Vignaradiata* L.) affected by Synthesized Zinc Oxide Nanoparticles. *Int. J. Curr. Eng. Technol.* **2014**, *4*, 3411.
45. Melo, M.A.S.; Guedes, S.F.F.; Xu, H.H.K.; Rodrigues, L.K.A. Nanotechnology-based restorative materials for dental caries management. *Trends Biotechnol.* **2013**, *31*, 459–467. [[CrossRef](#)]
46. Shionoya, S.; Yen, W.M. (Eds.) *Phosphor Handbook*; CRC Press: Boca Raton, FL, USA, 1998.
47. Berger, L.I. *Semiconductor Materials*; CRC Press: Boca Raton, FL, USA, 1997.
48. Vanheusden, K.; Warren, W.L.; Seager, C.H.; Tallant, D.R.; Voigt, J.A.; Gnade, B.E. Mechanisms behind green photoluminescence in ZnO phosphor powders. *J. Appl. Phys.* **1996**, *79*, 7983–7990. [[CrossRef](#)]
49. Fan, X.M.; Lian, J.S.; Zhao, L.; Liu, Y.H. Single violet luminescence emitted from ZnO films obtained by oxidation of Zn film on quartz glass. *Appl. Surf. Sci.* **2005**, *252*, 420–424. [[CrossRef](#)]
50. Brus, L. Electronic wave functions in semiconductor clusters: Experiment and theory. *J. Phys. Chem.* **1986**, *90*, 2555–2560. [[CrossRef](#)]
51. Phan, T.N.; Buckner, T.; Sheng, J.; Baldeck, J.D.; Marquis, R.E. Physiologic actions of zinc related to inhibition of acid and alkali production by oral streptococci in suspensions and biofilms. *Oral Microbiol. Immunol.* **2004**, *19*, 31–38. [[CrossRef](#)]

52. Giertsen, E. Effects of mouth rinses with triclosan, zinc ions, copolymer, and sodium lauryl sulphate combined with fluoride on acid formation by dental plaque in vivo. *Caries Res.* **2004**, *38*, 430–435. [[CrossRef](#)]
53. Turner, R.D.; Mesnage, S.; Hobbs, J.K.; Foster, S.J. Molecular imaging of glycan chains couples cell-wall polysaccharide architecture to bacterial cell morphology. *Nat. Commun.* **2018**, *9*, 1263. [[CrossRef](#)]
54. Villegas, N.A.; Compagnucci, M.J.S.; Aja, M.S.; Rocca, D.M.; Becerra, M.C.; Molina, G.F.; Palma, S.D. Novel antibacterial resin-based filling material containing nanoparticles for the potential one-step treatment of caries. *J. Healthc. Eng.* **2019**, *2019*, 6367919. [[CrossRef](#)]
55. Niu, L.; Fang, M.; Jiao, K.; Tang, L.H.; Xiao, Y.H.; Shen, L.J.; Chen, J.H. Tetrapod-like zinc oxide whisker enhancement of resin composite. *J. Dent. Res.* **2010**, *89*, 746–750. [[CrossRef](#)]
56. Hojati, S.T.; Alaghemand, H.; Hamze, F.; Babaki, F.A.; Rajab-Nia, R.; Rezvani, M.B.; Kaviani, M.; Atai, M. Antibacterial, physical and mechanical properties of flowable resin composites containing zinc oxide nanoparticles. *Dent. Mater.* **2013**, *29*, 495–505. [[CrossRef](#)]
57. Mahendra, R.; Ranjita, S. *Metal Nanoparticles in Pharma*, 1st ed.; Springer: Berlin/Heidelberg, Germany, 2017.
58. Zhang, L.; Jiang, Y.; Ding, Y.; Povey, M.; York, D. Investigation into the antibacterial behavior of suspensions of ZnO nanoparticles (ZnO nanofluids). *J. Nanoparticle Res.* **2006**, *9*, 479–489. [[CrossRef](#)]
59. Hamad, A.M.; Atiyea, Q.M. In vitro study of the effect of zinc oxide nanoparticles on Streptococcus mutans isolated from human dental caries. *J. Phys. Conf. Ser.* **2021**, *1879*, 022041. [[CrossRef](#)]
60. Qi, K.; Xing, X.; Zada, A.; Li, M.; Wang, Q.; Liu, S.; Lin, H.; Wang, G. Transition metal doped ZnO nanoparticles with enhanced photocatalytic and antibacterial performances: Experimental and DFT studies. *Ceram. Intern* **2020**, *46*, 1494–1502. [[CrossRef](#)]